The heat flux and the temperature gradient in the lower atmosphere

Chad W. Higgins,[1,2] Marc B. Parlange,[1,2] and Charles Meneveau[2,3]

Received 22 March 2004; revised 1 July 2004; accepted 9 August 2004; published 23 November 2004.

[1] Most parameterizations used in Large Eddy Simulations of the atmospheric boundary layer are based on the assumption that subgrid-scale fluxes are aligned against spatial gradients of transported quantities (down-gradient closures). Based on field experiments, we determine the distribution and most probable relative orientations of the subgrid-scale (SGS) heat flux relative to parameterizations based on the temperature gradient. We show that, under neutral and unstable atmospheric stability, the SGS heat flux most likely lies within the geometric span of the so called mixed tensor eddy diffusivity model. *INDEX TERMS:* 0312 Atmospheric Composition and Structure: Air/sea constituent fluxes (3339, 4504); 0350 Atmospheric Composition and Structure: Pressure, density, and temperature; 0394 Atmospheric Composition and Structure: Instruments and techniques; 0368 Atmospheric Composition and Structure: Troposphere—constituent transport and chemistry. **Citation:** Higgins, C. W., M. B. Parlange, and C. Meneveau (2004), The heat flux and the temperature gradient in the lower atmosphere, *Geophys. Res. Lett.*, *31*, L22105, doi:10.1029/2004GL020053.

[2] Large eddy simulation (LES) is a numerical technique that relies on a set of parameterizations for numerically unresolved quantities occurring at length-scales smaller than tens of meters [*Lilly*, 1967; *Mason*, 1994; *Lesieur and Metais*, 1996; *Meneveau and Katz*, 2000]. Classical Parameterizations [*Smagorinsky*, 1963; *Lilly*, 1967] are based on the assumption that subgrid-scale fluxes are aligned against spatial gradients of transported quantities down-gradient closures. Typically these parameterizations are tested by implementing them in model runs, and comparing the outcome of the simulations with available data. However, due to the integrated nature of model results (they combine effects of time integration schemes, accuracy of numerical discretizations, and methods of statistical averaging) such tests do not provide the needed insight into the physical soundness of the parameterization. A more direct approach, a-priori testing has been explored extensively in the context of engineering flows [*Clark et al.*, 1979; *Bardina*, 1980; *Liu et al.*, 1994] and in ABL turbulence [*Porté-Agel et al.*, 2001; *Sullivan et al.*, 2003]. In this approach, SGS quantities are measured from experimental data and directly compared with parameterizations. Here we present field observations that examine the flux-model alignments for the specific case of subgrid-scale (SGS) heat flux vectors in the lower atmosphere at length-scales relevant to LES. Individual components of the subgrid heat flux in the lower atmosphere have already been analyzed based on field data [*Porté-Agel et al.*, 1998], but without reaching conclusions about geometric alignment trends (*Porté-Agel et al.* [1998] used a 1-D filtering technique that is significantly less accurate than 2-D filtering used in the present work, see below). Atmospheric momentum flux statistics have been studied by *Porté-Agel et al.* [2001], *Horst et al.* [2004], and *Higgins et al.* [2003].

[3] In LES, the flux of heat (per unit heat capacity) caused by unresolved (SGS) motions occurring at scales smaller than a scale Δ is defined according to

$$q_i(\mathbf{x},t) = \widetilde{Tu_i} - \tilde{T}\tilde{u}_i \tag{1}$$

where u_i is the velocity vector, T is the temperature, and the tilde represents spatial filtering at the scale Δ. $\tilde{u}_i$ and $\tilde{T}$ are the filtered velocity and temperature fields that are numerically resolved in the LES model. The product $\widetilde{Tu_i}$, however, is not known since it depends upon small-scale fluctuations that are not computed explicitly. The closure problem in LES consists of expressing the vector $q_i(\mathbf{x},t)$ in terms of the resolved fields, such as $\tilde{T}(\mathbf{x},t)$ and $\tilde{u}_i(\mathbf{x},t)$. Classical parameterizations for $q_i(\mathbf{x},t)$ in LES are based on down temperature gradient closures. Specifically, the *Smagorinsky* [1963] eddy-diffusion parameterization reads:

$$q_i(\mathbf{x},t) = -\Gamma_\Delta \frac{\partial \tilde{T}}{\partial x_i}\left(\equiv q_i^{eddy}\right) \quad \text{where} \quad \Gamma_\Delta = \left(c_s^2 \mathrm{Pr}^{-1}\right)\Delta^2\left|\tilde{\mathbf{S}}\right| \tag{2}$$

The subgrid-scale eddy-diffusivity, Γ_Δ, contains $\left|\tilde{\mathbf{S}}\right| = \sqrt{2\tilde{S}_{ij}\tilde{S}_{ij}}$, the magnitude of the filtered strain rate tensor, $\tilde{\mathbf{S}} = \frac{1}{2}\left[\nabla u + (\nabla u)^T\right]$, and a dimensionless empirical coefficient ($c_s^2\ \mathrm{Pr}^{-1}$) (often written as the Smagorinsky constant (c_s^2) multiplied by an inverse subgrid-scale Prandtl number (Pr^{-1}).)

[4] The tensor eddy diffusivity (or nonlinear) model [*Leonard*, 1997; *Borue and Orszag*, 1998; *Kang and Meneveau*, 2002; *Martins Afonso et al.*, 2003] is given by

$$q_i(\mathbf{x},t) = c_{nl}\Delta^2 \frac{\partial \tilde{u}_i}{\partial x_k}\frac{\partial \tilde{T}}{\partial x_k}\left(\equiv q_i^{nl}\right) \tag{3}$$

where c_{nl} is the corresponding model coefficient and repeated subscripts are summed over, this can be shown mathematically [*Leonard*, 1997] by keeping the first term in an expansion of the filtered product $\widetilde{Tu_i}$ that appears in the definition of $\mathbf{q}$. Physically, the tensor eddy diffusivity produces a heat flux which is generally rotated with respect to the filtered temperature gradient (or $\mathbf{q}^{\mathrm{eddy}}$, hence the name

[1]Department of Geography and Environmental Engineering, Johns Hopkins University, Baltimore, Maryland, USA.
[2]Also at Center for Environmental and Applied Fluid Mechanics, Johns Hopkins University, Baltimore, Maryland, USA.
[3]Department of Mechanical Engineering, Johns Hopkins University, Baltimore, Maryland, USA.

0094-8276/04/2004GL020053$05.00

"tensor diffusivity"), in a manner that depends on the local flow field. Decomposing the velocity gradient tensor into its symmetric (strain-rate tensor $\tilde{\mathbf{S}}$) and rotational parts, and expressing the latter in terms of the filtered vorticity vector $\tilde{\mathbf{w}}$, the tensor eddy diffusivity heat flux can be written as

$$\mathbf{q}^{nl} = c^{nl}\Delta^2\left(\tilde{\mathbf{S}}\cdot\nabla\tilde{T} - \frac{1}{2}\tilde{\mathbf{w}}\times\nabla\tilde{T}\right). \quad (4)$$

Considering the coordinate system formed by the orthogonal eigendirections of the strain-rate tensor we can write $\tilde{\mathbf{S}} = \alpha\,\boldsymbol{\alpha}\boldsymbol{\alpha} + \beta\,\boldsymbol{\beta}\boldsymbol{\beta} + \gamma\,\boldsymbol{\gamma}\boldsymbol{\gamma}$, where α, β, γ are the three eigenvalues of $\tilde{\mathbf{S}}$, and $\boldsymbol{\alpha}$, $\boldsymbol{\beta}$, and $\boldsymbol{\gamma}$ are unit vectors in directions of the three eigendirections of $\tilde{\mathbf{S}}$. Then equation (4) is written as

$$\mathbf{q}^{nl} = c^{nl}\Delta^2\left[\alpha(\nabla_\alpha\tilde{T})\boldsymbol{\alpha} + \beta(\nabla_\beta\tilde{T})\boldsymbol{\beta} + \gamma(\nabla_\gamma\tilde{T})\boldsymbol{\gamma} - \frac{1}{2}\tilde{\mathbf{w}}\times\nabla\tilde{T}\right] \quad (5)$$

where $\nabla_\eta\tilde{T} \equiv \boldsymbol{\eta}\cdot\nabla\tilde{T}$ denotes temperature gradient in the $\boldsymbol{\eta}$-direction. Since the velocity field is divergence-free, $\alpha + \beta + \gamma = 0$ and the eigensystem can be ordered such that $\alpha > \beta > \gamma$ and $\alpha > 0$ (extensive eigen-direction), $\gamma < 0$ (contracting eigendirection), and β is either positive or negative (and smallest in magnitude). According to equation (5), $\mathbf{q}^{nl}$ contains four terms that cause $\mathbf{q}^{nl}$ to be rotated with respect to $\nabla\tilde{T}$. The first term in equation (5) shows that temperature gradients in the extensional directions of the flow lead to counter-gradient diffusion because $\alpha > 0$, while the third term is diffusive since $\gamma < 0$. These properties of the tensor eddy-diffusivity model have been already observed [*Leonard*, 1997]. The last term in equation (5) represents rotation of the temperature gradient to a direction normal to both the vorticity and temperature gradient.

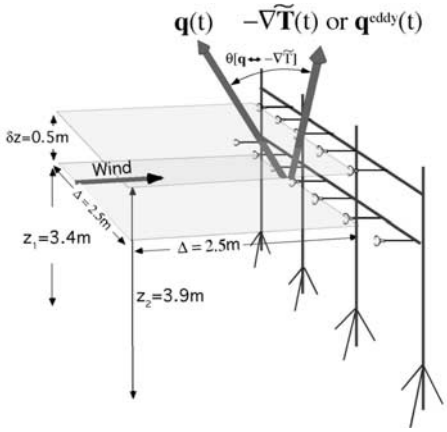

Figure 1. Sketch of the sonic anemometer array configuration for the Davis 99 experiment, with filtering scale Δ. Two horizontal arrays of three-dimensional sonic anemometers measuring the velocities and temperatures at 20 Hz, and at heights 3.4 m and 3.9 m, are orientated perpendicular to the mean flow. The field is a flat, bare soil field with 500 m of uninterrupted upwind fetch. Taylor's hypothesis is used to convert the temporal measurements, of velocity and temperature, to spatial measurements. The spatial data are then filtered on a scale $\Delta = 2.5$ m in the stream-wise and horizontal cross-stream directions. Spatial gradients of the filtered velocity and temperature are calculated with finite differences. These gradients, along with the filtered velocity and temperature fields, and their products, are then used to calculate the subgrid heat flux vector ($\mathbf{q}$, see equation (1)) and its parameterizations (e.g. $\mathbf{q}^{eddy}$, see equation (2)) which are drawn schematically.

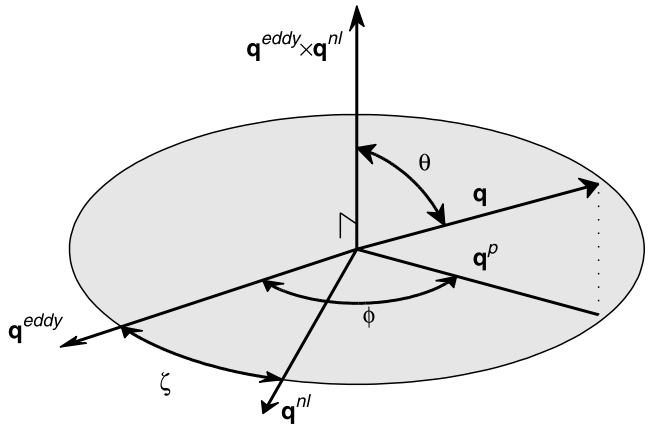

Figure 2. Sketch of the definitions of angles used in the data analysis. θ is the angle between the real SGS heat flux vector $\mathbf{q}$ and the normal to the plane spanned by the mixed model. ϕ is the angle between the projection of $\mathbf{q}$ onto the mixed model span ($\mathbf{q}^{\mathrm{p}}$) and the eddy diffusivity parameterization $\mathbf{q}^{eddy}$. ζ is the angle between $\mathbf{q}^{nl}$ and $\mathbf{q}^{eddy}$.

[5] A third approach, the so-called mixed model [*Bardina et al.*, 1980; *Zang et al.*, 1993; *Vreman et al.*, 1994], is a linear combination of equations (2) and (3):

$$q_i(\mathbf{x},t) = c\,\Delta^2\left[-|\tilde{\mathbf{S}}|\frac{\partial\tilde{T}}{\partial x_i} + \lambda\frac{\partial\tilde{u}_i}{\partial x_k}\frac{\partial\tilde{T}}{\partial x_k}\right] \quad \left(\equiv q_i^{mix}\right) \quad (6)$$

Mixed models have already been used for the momentum flux with success in various applications [*Katz and Meneveau*, 2000].

[6] Present results are obtained from geometric and statistical analysis of the "Davis99" data set described in detail by *Porté-Agel et al.* [2001]. Time series of the three-component wind velocity vector and the temperature in the atmospheric surface layer were obtained in Davis California during the summer of 1999. Signals were recorded at 20 Hz, using two horizontal arrays of 3-dimensional sonic anemometers. The arrays, separated vertically by $\delta z = 0.5$ m, were arranged to obtain the wind velocity and temperature field along two horizontal lines. The lower array, located at a height of $z_1 = 3.4$ m, contained seven anemometers, while the upper array, at a height of $z_2 = 3.9$ m, contained five sonic anemometers (see Figure 1).

[7] In this study, the data are broken into two groups based on the value of z/L denoted by groups (a) and (b) respectively. The Obukhov length is defined as $L = \frac{-\langle T\rangle u_*^3}{\kappa g\langle T'w'\rangle}$ (where, $u_* = \sqrt{-\langle u'w'\rangle}$ is the friction velocity). Primes denote fluctuating quantities, $\langle\ldots\rangle$ represents averaging over time, κ (=0.4) is von Kármán's constant and g is the acceleration of gravity. Group (a) consists of a 25-minute time segment taken on June 6, 1999 at 6:30 PM in which $|z/L| < 0.02$. During the sample period, the mean temper-

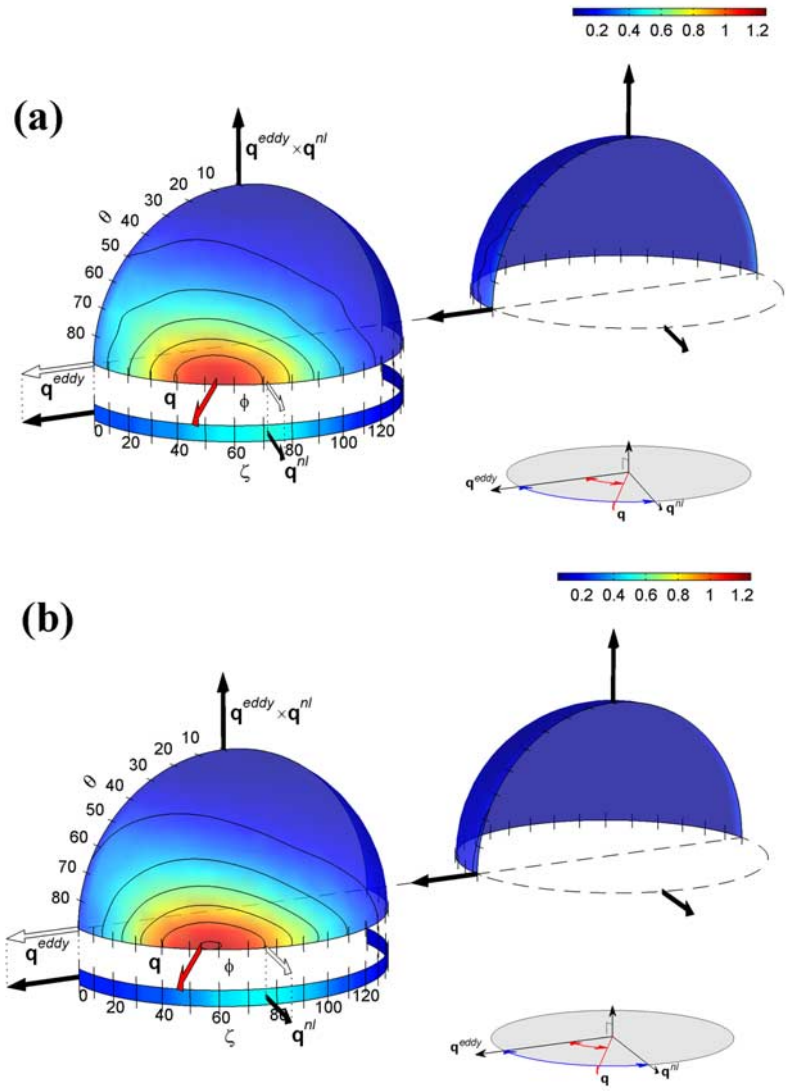

Figure 3. Joint PDF of the angles (θ,ϕ) plotted on half the unit sphere (note the PDF is symmetric about the equator) for data sets (a) and (b). The red regions on the sphere denote the highest likelihood of the measured heat flux ($\mathbf{q}$) orientation. The measured heat flux is observed to be oriented most often near the equatorial plane. Together $\mathbf{q}^{eddy}$ and $\mathbf{q}^{nl}$ define a subspace where $\mathbf{q}$ is most often oriented. The PDF of ζ, the angle between $\mathbf{q}^{nl}$ and $\mathbf{q}^{eddy}$, is shown along the bottom strip. The front of the unit sphere contains the peak of the PDF, the posterior of the unit sphere (pointing opposite to the direction of $\mathbf{q}^{nl}$) shows very low probability of orientation. A sketch summarizing the most probable relative orientation of $\mathbf{q}$, $\mathbf{q}^{nl}$ and $\mathbf{q}^{eddy}$ for each atmospheric stability regime is also presented.

ature decreased by 0.5 C. We measured the rate of cooling by linear regression and found that at that time the atmosphere was cooling at a rate of $\sim$1 C/hour. In Group (b), $z/L < -0.5$. This corresponds to roughly 13 hours of data.

[8] To evaluate the SGS heat fluxes and the temperature gradients, the data are filtered in both the cross-stream and stream-wise directions at a scale of $\Delta = 2.5$ m. This scale is smaller than the measurement height and falls near the transition between the inertial range and the integral scale of turbulence, a common situation in LES modeling near the ground [*Porté-Agel et al.*, 2001]. The fluctuations in the stream-wise direction are filtered with a Gaussian filter in which Taylor's hypothesis is invoked to convert temporal measurements of velocity and temperature into stream-wise measurements. With a typical wind speed of 6 m/s and Δ = 2.5 m this steam-wise filtering corresponds to a time filtering of 0.42 s. Filtering in the cross-stream direction is performed with a box filter by averaging the signals from the anemometers along each array [*Porté-Agel et al.*, 2001]. No filtering is done in the vertical direction, thus 2-D filtering is used as a surrogate to 3-D filtering in this analysis. The accuracy of this filtering technique was investigated in *Tong et al.* [1998] with LES data. They showed a 10–14% difference in variances between the 2-D filtered and 3-D filtered variables of interest. Many other studies [*Horst et al.*, 2004; *Sullivan et al.*, 2003] use a similar filtering technique. Figure 1 shows the implied filter planes that are sampled discretely by the sonic anemometers. Gradients are calculated using finite differencing over a distance of $\delta z = \Delta/5 = 0.5$ m in all three directions.

[9] To better understand the relationship between $\mathbf{q}$ and the mixed model, we consider the alignments of the real SGS heat flux relative to the "mixed model span", defined as the plane containing the two vectors $\mathbf{q}^{eddy}$ and $\mathbf{q}^{nl}$ (this is a well defined space since these two vectors are highly misaligned, see below). A sketch of the geometry and definition of angles used in this analysis is presented in Figure 2. The normal to the mixed model span is given by $\mathbf{q}^{eddy} \times \mathbf{q}^{nl}$. The projection, $\mathbf{q}^{\mathrm{p}}$, of the measured heat flux onto the plane spanned by the mixed model is the portion of the SGS heat flux that can be expressed by the mixed model. Figure 3 shows the measured joint probability density function of $\theta = \cos^{-1}\frac{\left(\mathbf{q}^{eddy} \times \mathbf{q}^{nl}\right)\cdot\mathbf{q}}{|\mathbf{q}^{eddy} \times \mathbf{q}^{nl}||\mathbf{q}|}$ and $\phi = \cos^{-1}\frac{\mathbf{q}^{eddy}\cdot\mathbf{q}^{p}}{|\mathbf{q}^{eddy}||\mathbf{q}^{p}|}$ plotted on the unit sphere for both data sets (a) and (b) respectively. This joint PDF quantifies the relative frequency of orientations of the measured SGS heat flux relative to the model defined coordinates. In addition, a single PDF of $\zeta[\mathbf{q}^{eddy} \leftrightarrow \mathbf{q}^{nl}]$ is shown at the bottom of each plot to characterize the alignment of the tensor eddy diffusivity vector with respect to the eddy-diffusion vector. We have quantified the level of statistical convergence of the PDFs by computing running averages. The PDF counts have been found to be very well converged, with uncertainties of less than 5%. Also, the autocorrelation functions of SGS heat fluxes and temperature gradients have been computed from the data. They decay to zero for time delays over about 2 seconds (i.e., about 4 times the filter scale). Thus, SGS phenomena studied in this paper occur on fast time-scales allowing statistics collected over 20-minute periods to be statistically converged.

[10] In both cases of z/L ranges (a) and (b) considered, the most likely orientation of the measured SGS heat flux does not coincide with the orientation of either the eddy diffusivity $\mathbf{q}^{eddy}$ (Smagorinsky) or the tensor eddy diffusivity model $\mathbf{q}^{nl}$ (see Figure 3). However, the measured SGS heat flux aligns closely with the span of the mixed model (the equatorial plane in Figures 3a and 3b). Hence, the linear combination of $\mathbf{q}^{nl}$ and $\mathbf{q}^{eddy}$ defines a plane that describes well the most likely orientations of the SGS heat flux, independent of the parameter z/L. Note that at the peak the probability density is $\sim$1.2, whereas a random orientation would imply a probability density of 0.16.

[11] Of course one can argue that $\mathbf{q}^{nl}$ provides a useful vector complement to $\nabla\tilde{T}$ in a mixed parameterization, because it contains two terms (the first and last in equation (5)) that are very likely to be perpendicular to $\nabla\tilde{T}$. This is a consequence of the following two observations: (1) As we have verified from the data, the filtered temperature gradient tends to align fairly well with the contracting eigendirection $\boldsymbol{\gamma}$ of the velocity field (possibly because iso-temperature surfaces are brought together in the direction of converging local streamlines). (2) The vorticity vector in turbulence tends to align with the intermediate eigenvector direction $\boldsymbol{\beta}$ [*Ashurst et al.*, 1987; *Tao et al.*, 2002; *Higgins et al.*, 2003]. A similar argument holds if the eigenvector ordering proposed by *Andreotti* [1997] and *Horiuti* [2003] is used. It follows that the first and last terms in equation (5) align with $\boldsymbol{\alpha}$, i.e., perpendicular to $\boldsymbol{\gamma}$ and likely perpendicular to $\nabla\tilde{T}$. However, the observation that $\mathbf{q}$ lies in the plane spanned by $\mathbf{q}^{nl}$ and $\nabla\tilde{T}$ is not trivial since $\mathbf{q}$ is a three-dimensional vector that could, in general, lie preferentially outside the plane spanned by the mixed model. In that case one would need a third independent basis vector in a more complicated parameterization. We also remark that the alignment with the mixed model plane is consistent with a recent theoretical calculation based on the Kraichnan advection model [*Martins Afonso et al.*, 2003].

[12] Present conclusions on the alignment of the subgrid-scale heat flux have been obtained under near neutral atmospheric stability and at heights above the ground with length-scales that are relevant to LES. Details of the most likely relative orientation within the mixed model span may depend heavily on flow conditions, dependencies that warrant further experimental studies. As present results show, such studies based on field experimental data in the lower atmosphere augment what can be learned from the otherwise limited computational trial-and-error tests of parameterizations commonly used in geophysical flow modeling. These studies could lead to the increased trustworthiness of LES and its predictions of atmospheric boundary layer dynamics, and to concomitant improvements in boundary layer parameterizations used in weather forecasting and global scale models.

[13] **Acknowledgments.** We thank W. Brutseart, S. Chen, T. Haine, and M. Hilpert for their helpful comments and suggestions. The data used in this work were collected jointly with F. Porté-Agel, W. Eichinger, and M. Pahlow. We are grateful to them and to R.H. Shaw for his help in the Davis99 field campaign. Supported in part by a grant from the National Science Foundation (NSF-ATM-0130766).

References

Andreotti, B. (1997), Studying Burgers' Models to investigate the physical meaning of the alignments statistically observed in turbulence, *Phys. Fluids*, *9*(3), 735–742.

Ashurst, W. T., A. R. Kerstein, R. M. Kerr, and C. H. Gibson (1987), Alignment of vorticity and scalar gradient with strain rate in simulated Navier-Stokes turbulence, *Phys. Fluids*, *30*, 2343–2353.

Bardina, J., J. H. Ferziger, and W. C. Reynolds (1980), Improved subgrid scale models for large eddy simulation, *AIAA Pap.*, *80–1357*.

Borue, V., and S. A. Orszag (1998), Local energy flux and subgrid-scale statistics in three-dimensional turbulence, *J. Fluid Mech.*, *366*, 1–31.

Higgins, C. W., M. B. Parlange, and C. Meneveau (2003), Alignment trends of velocity gradients and subgrid-scale fluxes in the turbulent atmospheric boundary layer, *Boundary Layer Meteorol.*, *109*, 59–83.

Horiuti, K. (2003), Roles of non-aligned eigenvectors of strain-rate and subgrid-scale stress tensors in turbulence generation, *J. Fluid Mech.*, *491*, 65–100.

Horst, T., J. Kleissl, D. Lenschow, C. Meneveau, C. H. Moeng, M. B. Parlange, P. P. Sullivan, and J. C. Weil (2004), HATS: Field observations to obtain spatially-filtered turbulence fields from crosswind arrays of sonic anemometers in the atmospheric surface layer, *J. Atmos. Science*, *61*, 1655–1581.

Kang, H. S., and C. Meneveau (2002), Universality of large eddy simulation model parameters across a turbulent wake behind a heated cylinder, *J. Turbulence*, *3*, 032 (http://jot.iop.org/).

Leonard, A. (1997), Large eddy simulation of chaotic convection and beyond, *AIAA Pap.*, *97–0204*, 8 pp.

Lesieur, M., and O. Metais (1996), New trends in large-eddy simulations of turbulence, *Ann. Rev. Fluid Mech.*, *28*, 45–82.

Lilly, D. K. (1967), The representation of small-scale turbulence in numerical simulation experiments, *Proceedings, IBM Scientific Computing Sympposium on Environmental Sciences*, November 14–16, 1966, Thomas J. Watson Research Center, Yorktown Heights, N.Y., edited by H. H. Goldstein, IBM Form No.320-1951, pp. 195–210.

Liu, S., J. Katz, and C. Meneveau (1994), On the properties of similarity subgrid-scale models as deduced from measurements in a turbulent jet, *J. Fluid Mech.*, *275*, 83.

Martins Afonso, M. M., A. Celani, R. Festa, and A. Mazzino (2003), Large-eddy-simulation of passive scalar turbulence: A systematic approach, *J. Fluid Mech.*, *496*, 355–364.

Mason, P. J. (1994), Large eddy simulation: A critical review of the technique, *Quart. J. Roy. Metero. Soc.*, *120*, 1–26.

Meneveau, C., and J. Katz (2000), Scale-invariance and trubulence models for large-eddy simulation, *Annu. Rev. Fluid Mech.*, *32*, 1–32.

Piomelli, U., P. Moin, and J. H. Ferziger (1988), Model consistency in large eddy simulation of turbulent channel flows, *Phys. Fluids*, *31*, 1884–1891.

Porté-Agel, F., C. Meneveau, and M. B. Parlange (1998), Some basic properties of the surrogate subgrid-scale heat flux in the atmospheric boundary layer, *Boundary Layer Meteorol.*, *88*, 425–444.

Porté-Agel, F., M. B. Parlange, C. Meneveau, and W. E. Eichinger (2001), A priori field study of the subgrid-scale heat fluxes and dissipation in the atmospheric surface layer, *J. Atmos. Sci.*, *58*, 2673–2697.

Smagorinsky, J. (1963), General circulation experiments with primitive equations, *Mon. Weather Rev.*, *91*, 99–164.

Tao, B., J. Katz, and C. Meneveau (2002), Statistical geometry of subgrid-scale stresses determined from holographic particle image velocimetry measurements, *J. Fluid Mech.*, *457*, 35–78.

Tong, C. N., J. C. Wyngaard, S. Khanna, and J. G. Brasseur (1998), Resolvable- and subgrid-scale measurement in the atmospheric surface layer: Technique and issues, *J. Atmos. Sci.*, *55*(20), 3114–3126.

Vreman, B., B. Geurts, and H. Kuertein (1994), On the formulation of the dynamic mixed subgrid-scale model, *Phys. Fluids*, *6*, 4057–4059.

Zang Y., R. L. Street, and J. Koseff (1993), A dynamic mixed subgrid-scale model and its application to turbulent recirculating flows, *Phys. Fluids*, *5*, 3186–3196.

C. W. Higgins and M. B. Parlange, Department of Geography and Environmental Engineering, Johns Hopkins University, Baltimore, MD 21218, USA. (chad@jhu.edu)

C. Meneveau, Department of Mechanical Engineering, Johns Hopkins University, Baltimore, MD 21218, USA.